International Journal of Industrial Electronics, Control and Optimization © 2020 IECO
Vol. 3, No. 1, pp. 19-26, jan (2020)

Static Eccentricity Fault Diagnosis in a Cylindrical Wound-Rotor Resolver

[1]Shima Tavakoli, [2] †Zahra Nasiri-Gheidari

[1]Department of Electrical and Computer Engineering, Islamic Azad University, Science and Research Branch, Tehran, Iran
[2] Electrical Engineering Department, Sharif University of Technology, Tehran, Iran

ABSTRACT

Static eccentricity (SE) is an intrinsic fault existing in both faulty and newly made resolvers. The late diagnosis of SE causes severe damages to mechanical parts of resolver such as bearings, cores, and even windings, in addition to wrong position estimation. However, so far, fault diagnosis has not been investigated for any resolver. In this paper, SE fault diagnosis is discussed for a sample wound-rotor (WR) cylindrical resolver. Time stepping finite element method (TSFEM) is used to simulate the resolver, and its accuracy is validated by a comparison between the results of simulation and experimental tests. Then, some fault indices are defined to diagnose the SE fault occurrence, and its magnitude is predicted using Fast Fourier transform (FFT). Finally, to ensure that indices are unique, the performance of the studied resolver is evaluated under other types of faults including Dynamic Eccentricity (DE) and Short-circuit (SC) that may excite the same indices.

Article Info

Keywords:
Dynamic Eccentricity, Fault Diagnosis, Short Circuit, Static Eccentricity, TSFEM, Wound-Rotor Resolver

Article History:
Received 2019-06-08
Accepted 2019-06-16

I. INTRODUCTION

High-performance control of inverter-driven electrical machines needs to be aware of exact rotor position. Therefore, researchers are encouraged to find the best position sensing methods, considering their required accuracy, cost-effectiveness, and reliability.

Resolvers are electromagnetic position sensors which have prevailed over optical encoders. Although, encoders are the most common, low price sensors [1, 2] their application in harsh, polluted, vibrational environments is questioned [2-4] Resolvers resemble two-phase high-frequency ac excited generators and come in two major types of Wound Rotor (WR) and Variable Reluctance (VR). The pros and cons of each type are discussed in [2, 5]. According to [6], VR resolvers can compete with wound rotor resolvers economically due to lack of winding on their rotor. However, they have lower accuracy in comparison to WR types, especially in low pole applications and under mechanical faults [5, 7].

A resolver is mechanically coupled to an electric machine; hence, any mechanical fault of the machine would be transferred to the resolver. Those faults cause position error increment in addition to mechanical friction and damages.

Effect of eccentricity faults on the performance of resolvers has been the subject of many research papers [1] [8-11]. However, their fault diagnosing methods are not discussed yet. All fault diagnosis methods are divided into two signal-based and model-based categories. The former is the most common method for fault diagnosis of electric machines which deploys harmonic frequency content of the signals such as phase current[1] or electromagnetic torque to define the

†Corresponding Author: znasiri@sharif.edu
Tel: +9821 6616 4389, Fax: +9821 6602 3261, Electrical Engineering Department, Sharif University of Technology

[1] Current signature

indices for fault detection [12-17]. Nevertheless, it is better not to choose invasive signals such as radial force, air gap flux density, and cogging torque for experimental fault diagnosis [13]. Ebrahimi and et al. have found a logical relationship between harmonics changes and the emergence of new harmonics' frequency and different types of eccentricity in [18]. Hence one can obtain a frequency pattern of each type of fault algorithm to detect fault continuously by a computer connected signal sampler. Also, many have discussed the accuracy of fault detection for different types of rotors [19] and loading conditions [20, 21]. According to Ebrahimi[13], a suitable fault diagnosis index is one which is able to detect fault occurrence, its type, and magnitude accurately. The amplitude of the phase current in resolvers is microscopic; therefore, the electromagnetic torque is negligible, too. As a consequence, they are not suitable candidates for resolver's fault diagnosis.

In this paper, static eccentricity is detected based on output windings' voltage and flux density signals indices for a sample WR resolver. Then, the uniqueness of all indices is verified from dynamic eccentricity and short-circuit faults. Once the indices are verified, the magnitude of the fault is calculated by interpolation between exponentially increasing data points. Voltage and air gap flux density signals are chosen because of their successful performance examination among many other signals. All the simulations are done using time stepping finite element method, and the experimental test on the studied resolver is used to validate the simulation accuracy in the healthy state before applying different faults.

II. Structure of Studied Resolver

The studied resolver has two poles cylindrical wound rotor structure. Rotor has a variable turn, on-tooth winding. The stator has 11 slots that contain 2-phase variable turn, on-tooth windings which are known as signal windings. Fig. 1 (a) shows the schematic of the studied resolver, and Table 1 presents its electrical and mechanical parameters.

III. Simulation of the Studied Resolver

The accurate model of a faulty machine is the first stage, which has a considerable impact on accurate fault detection. Hence as shown in Fig. 1 (b), the Finite Element Method is used for simulating the resolver due to its high accuracy. However, there are some considerations that should be considered in the finite element simulation of resolver, including excitation type, setting time step, and stop time of simulation, assigning mesh operations, and selecting the solver that is discussed in detail in [22]. In this paper, Ansys-Electromagnetic Suit 17.1 software is used for simulations. The excitation winding is on the rotor and fed using a high-frequency sinusoidal voltage. The rotor is rotated in a constant speed, and the induced voltages on the signal windings that are located on the stator are given as presented in **Fig. 2**.

Table 1. Resolver properties

Parameters	unit	Value
Mechanical speed	rpm	300
Excitation voltage	V	5
Excitation frequency	Hz	4000
Rotor slots	-	20
Stator slots	-	11
Inner/outer rotor diameter	mm	23.53/31.99
Inner/outer stator Diameter	mm	34.13/ 45.96
Stator teeth width	mm	7.12
Rotor teeth width	mm	2.65
Stator slot height	mm	6.7
Rotor slot height	mm	6

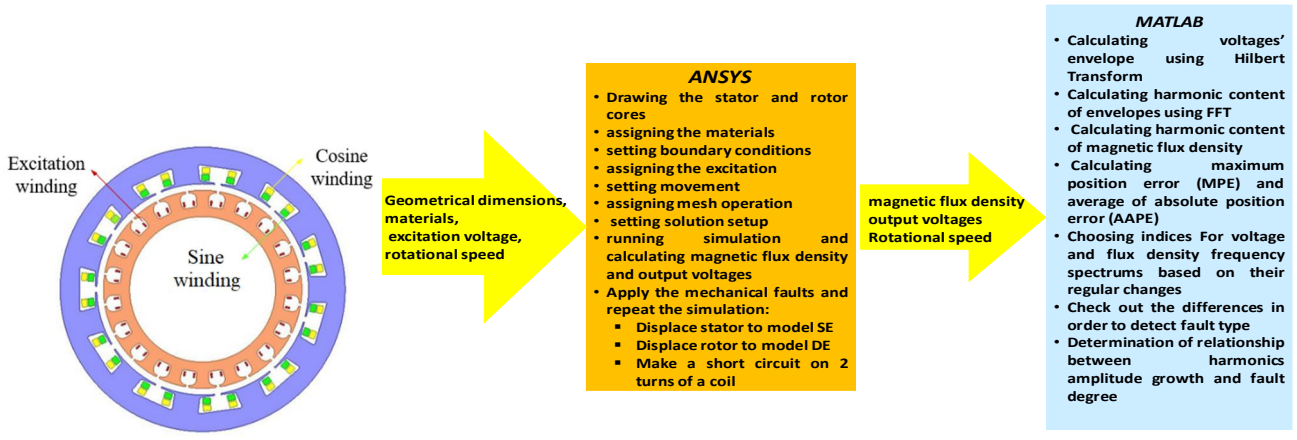

(a) (b)

Fig. 1. (a) The schematic of the studied resolver (b) Schematic flowchart of the simulation procedure

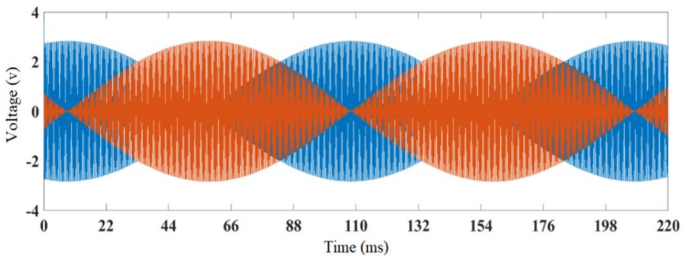

Fig. 2. Output signal windings voltage waveforms

The equations below show the output perpendicular voltage signals:

$$V_s = V \sin(2\pi f) \sin\theta$$
$$V_c = V \sin(2\pi f) \cos\theta \quad (1)$$

where V is the amplitude of the induced voltage, f is the excitation frequency, and θ is the angular position of the rotor that can be calculated through:

$$\theta = \arctan\left(\frac{V_s}{V_c}\right) \quad (2)$$

In order to use the sine and cosine voltage for this purpose, it is necessary to obtain their envelope, because of their high-frequency oscillating content. The signals envelope is obtained using the Hilbert transform in Matlab. Then, the harmonic content of the envelopes is determined, and the voltage amplitude and total harmonic distortion (THD) of envelopes are calculated. Afterward, the inverse tangent of the envelopes' ratio is used to calculate the rotor position. Comparing the calculated rotor position with the reference position gives the position error. The reference position in the simulations is also calculated using the mechanical speed of resolver. While in the experimental test, it is measured using the reference position sensor that is an optical encoder. Then the Maximum position error (MPE) and the average of absolute position error (AAPE) as the best factors for determining the accuracy of the resolvers can be calculated [22]. The performance characteristic of the studied resolver is reported in Table 1.

IV. Validation of Resolver Model Using Experimental Results

In this section, the wound-rotor resolver is constructed, and TSFEM experimental test is performed on it to make sure of the simulation accuracy. The stator and rotor and the test set-up are shown in Fig. 3Fig. 4, respectively.

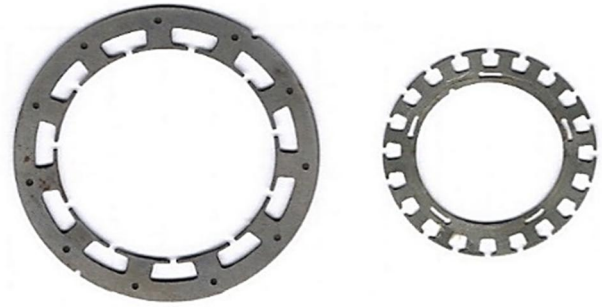

Fig. 3. Core sheets of studied resolver:(a) Stator sheet and (b) Rotor sheet

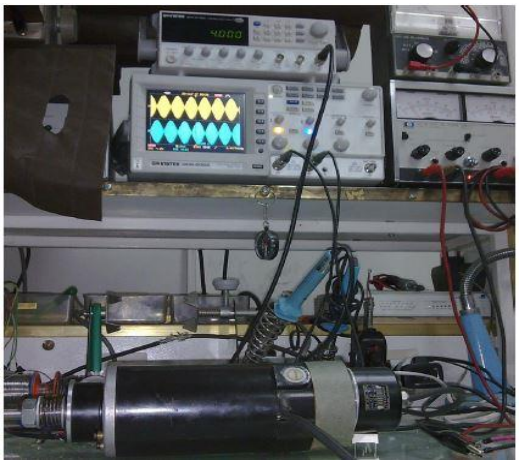

Fig. 4. Experimental test set-up of the studied resolver

In the test set-up, the understudy resolver is coupled with a DC motor. While a programmable 18-bit optical encoder, as a reference sensor, detects the real rotor position. Also, a digital oscilloscope is used to measure and save the output voltages. Induced voltage traced by the oscilloscope is shown in Fig. 5. The voltage signal information is recorded by flash memory, and further calculations are done in MatLab software. Experimental test's results show that the THD of voltages' envelope is 0.1660% while its value is estimated at 0.1569% using TSFEM. Also, the Average of Absolut Position Error (AAPE) is calculated equal to 0.0773º and 0.0734º for experimental and simulation results, respectively. More details are reported in Table . The difference between the simulation and experimental results are about 5%. Accordingly, one can trust the validity of the simulation accuracy to apply different faults and investigate their effect on the simulation model.

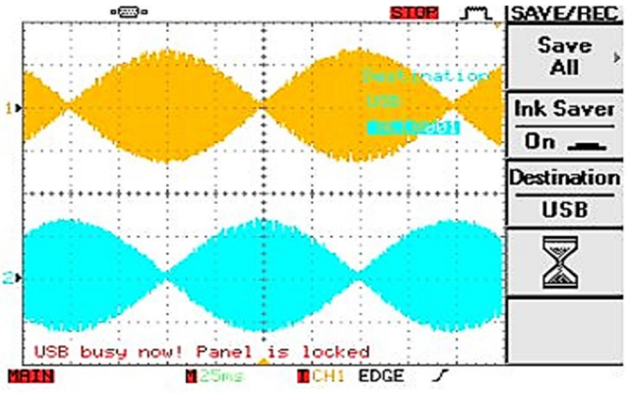

Fig. 5. The measured voltage waveforms

Table II. Resolver simulation results in healthy state

	Amplitude (V)	THD (%)	MPE (Deg.)	AAPE (Deg.)
Sine	2.0117	0.1569	0.2075	0.0735
Cosine	2.0163	0.1547		

Based on the fault indices evaluation procedure suggested in [23], every index proposed for fault diagnosis should be able to detect fault occurrence as the first step. If the index could clarify the fault type from other possible faults and determine the fault severity, then one can nominate the index for fault diagnosis safely.

V. INDEXING SE FAULT

One can apply static/dynamic eccentricity on the healthy model of resolver by displacing stator/rotor axis from their original place, respectively. The amount of both a displacement is reported in Table III. Static eccentricity percentage corresponds to stator axis displacement value. This value can be calculated by (3):

$$\mathrm{SE} = \frac{g_{max} - g_{min}}{2g_0} \tag{3}$$

Where g0 is the air gap length and $g_{max} = g_0 - g_{min}$. gmax and gmin are the maximum and the minimum air gap lengths in case of stator axis displacement (SE). Air gap length of the healthy resolver is 1.07 mm for the studied resolver.

Table III.

Eccentricity percentages applied to the simulated model

Percentage	10%	20%	30%	40%	50%
Displacement (mm)	0.107	0.214	0.321	0.428	0.535

The frequency spectrum of any signal might reveal the fault trace on its content. One can detect fault by a precise investigation on the harmonics changes which are able to reveal fault occurrence, its type, and magnitude. Hence the bar graph of the frequency spectrum of the output sine voltage is generated and illustrated in Fig. 6 using a logarithmic scale for the healthy resolver using fast Fourier transform on its envelope. Every harmonic component contains a distinct frequency which is a multiple of the fundamental frequency of 5 Hz.

$$n_s = \frac{120f}{p} = 300 \rightarrow \mathrm{f}=5\mathrm{Hz} \tag{4}$$

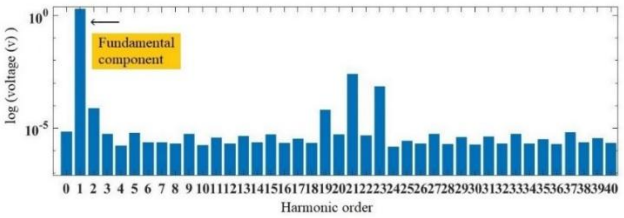

Fig. 6. The logarithmic frequency spectrum of voltage envelope

A. DIAGNOSIS USING THE VOLTAGE SIGNAL

In order to realize the effect of static eccentricity on the voltage harmonic components, the fault is applied to the healthy simulation model according to the values of Table . The frequency spectrum of output sinusoidal voltage in the same coordinate system is shown in Fig.7 for both healthy and 50% SE affected signal.

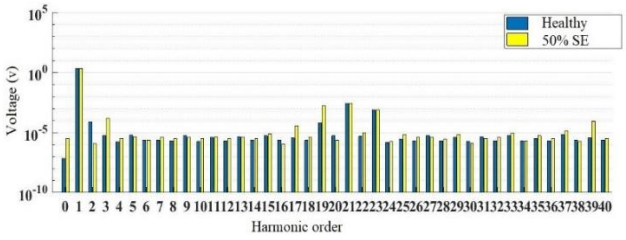

Fig. 7. Sine winding harmonic components under the healthy and static fault state

The amplitude of most of the harmonic components are increased as the stator axis is displaced, and the air gap is asymmetric subsequently.

The same work is done for every single SE fault percentage. By scrutinizing all the components changes during the fault severity increment, one can recognize the components, which have significant incremental changes that notify the fault. These components are listed in Table IV. The variation of the harmonic components versus SE percentage is shown in Fig.8 . As can be seen, the 19th harmonic component is the clearest one, which contains a frequency of 95 Hz. By fitting a curve on the component's amplitude, both the eccentricity occurrence and its magnitude can be found out. It should be mentioned that despite significant variations of the third harmonic amplitude, it is not an acceptable index because it is excited in almost all type of faults.

The other harmonic components vulnerability will be discussed in section 6.

Table IV.
Voltage envelope indices for static eccentricity

Winding	Harmonics order
Sine winding	3 ,17, 19, 39, 41, 43
Cosine winding	17, 19, 39, 41, 61

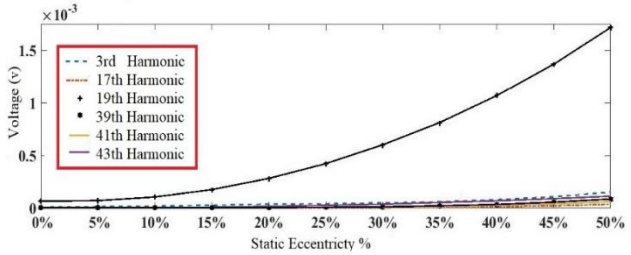

Fig. 8. Exponential increment in the amplitude of harmonics of flux density versus static eccentricity percentage

B. Diagnosis Using Flux Density Signal

The air gap length reduction in the first half cycle and increment in the other half due to static eccentricity causes its asymmetry. Subsequently, air gap flux density changes are erratic. As it is shown in Fig.9, flux density reduces in the first cycle and increases in the other, while static eccentricity increases.

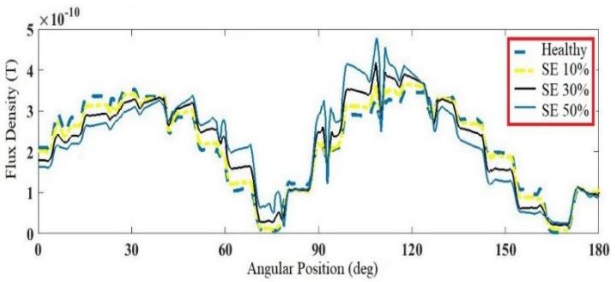

Fig. 9. Air gap flux density waveform under different static eccentricity values

Flux density bar graph of the frequency spectrum is drawn in Fig. 11 for three healthy and faulty state of static eccentricity. Just like the voltage signal, by securitizing the components changes, those that reveal SE are reported in Table V.

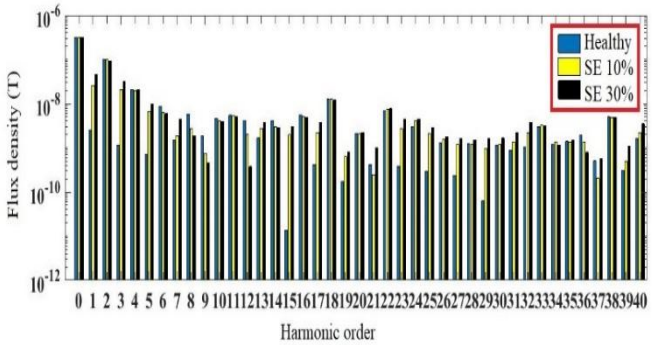

Fig. 10.The frequency spectrum of the air gap flux density signal in the healthy state and under static eccentricity states.

Table V.
flux density amplitude indices for static eccentricity

	Harmonic order
Odd harmonics	1,3,5,31,39,47,67,71,73
Even harmonics	32,40,42,56,64,66,88

VI. Uniqueness Verification of SE Fault Indices

As mentioned earlier, one can recognize SE fault using cited harmonic components. Nevertheless, the likelihood of the same effect under other types of faults necessitates evaluating them too, in order to identify SE uniquely. Dynamic eccentricity (DE) is intrinsically similar to SE, but unlike SE, it's the rotor's axis that varies from the two other axes.

The effect of short-circuit in excitation winding resembles the static and dynamic eccentricity; hence in order to verify static eccentricity from short-circuit, 2 turns of a 46 turn coil of the excitation winding are shorted, and its effect is investigated in the simulation environment. It is worth to mention that the eventuality of short-circuiting (SC) in the studied resolver is high due to fragile 0.060 mm and 0.100 mm copper wires used in signal and excitation windings, respectively.

The next two sections deal with the dynamic eccentricity and short-circuit effects on both voltage and flux density signals.

A. Voltage Signal Indices Verification

In this section, dynamic eccentricity is applied to the healthy model of the resolver. Resolver's rotor axis is displaced according to the values of Table 3. One can see the harmonics amplitude deviation under healthy and 50% dynamic eccentricity condition in Fig.11.

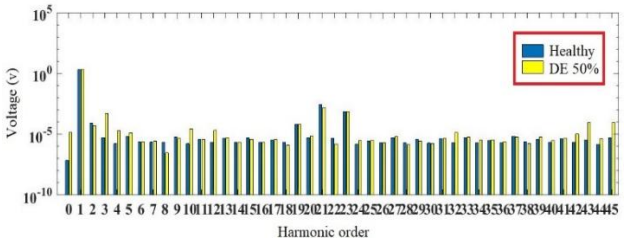

Fig. 11. The frequency spectrum of the voltage signal in the healthy state and under dynamic eccentricity states

Doing the same investigation for the harmonic components of voltage signal under different dynamic eccentricity percentages reveals those that their amplitude increase exponentially during faults percentage increment. Some harmonics amplitude increment vs. the dynamic eccentricity percent is such a regular one which enables to predict the dynamic eccentricity magnitude by intra-extrapolation. These harmonics are found by accurate assessment of all harmonics and are reported in Table VI.

In order to recognize eccentricity from short-circuit fault, two turns of one of the excitation winding's coils which contain 46 turns are shorted in the simulation environment. Most of the harmonic components amplitude change except some, which can help fault type recognition as they act differently. Both indices

for dynamic eccentricity and short-circuit are reported in Table VI.

Table and Table both show the harmonic components that can be used as each fault indices in voltage envelope. Comparing the value of these harmonics in both healthy and faulty states reveals the fault occurrence. Also, the magnitude of the fault can be realized using interpolation methods for their exponential equations. For instance, one can see the third and 43rd harmonic of sinusoidal voltage under dynamic eccentricity which supports this idea in Fig.12.

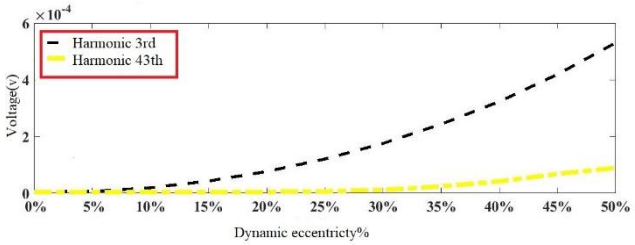

Fig. 12. The increment of candidate harmonics for dynamic eccentricity diagnosis

The order equation of these two harmonics are as below:

$$V = (2.3782\times10^{-9})x^3 - (1.186\times10^{-7})x^2 + (2.8928\times10^{-6})x + 2.5038\times10^{-6}$$
$$V = (-9.544\times10^{-11})x^3 + (6.0926\times10^{-8})x^2 - (6.6426\times10^{-8})x + 4.126\times10^{-6} \quad (4)$$

The importance of eccentricity type recognition gets highlighted as one must displace the stator or rotor axis back to their real position in order to prevent windings or even cores friction. This would be feasible in case of using unique, uncommon components for each case. In other words, using different harmonic components that are excited uniquely only by one type of fault, helps to recognize the fault correctly and fix the device properly to prevent repeating the fault.

Table VI.voltage envelope indices for dynamic eccentricity and short-circuit

	DE	SC
Sine winding	3, 43	all except 19,21, 23
Cosine winding	2, 45	all except 19,21,23

For example, the 45th harmonic component can denote the fault type uniquely. This harmonic component is excited only by DE fault and can help to find out the fault occurrence, its type and amount of rotor axis displacement. **Error! Reference source not found.** shows the 45th harmonic amplitude, which has a monotonic exponential growth as DE fault increases.

Table VII. The amplitude of 45th harmonic of voltage envelope versus DE percentage increment

Healthy	10%	20%	30%	40%	50%
0.539 ×10^-5	0.811 ×10^-5	2.02 ×10^-5	4.04 ×10^-5	6.2 ×10^-5	9.52 ×10^-5

B. FLUX DENSITY SIGNAL INDICES UNIFICATION:

The length of the air gap transiently changes over time as DE happens. Thus in the first half cycle, there is an abnormal increment, unlike the average reduction in the second half cycle of rotation when fault percentage is more than 40%. Fig.13 shows how DE effects on the air gap flux density during the two half cycles.

Using FFT for the flux density signal, the harmonic components changes are obtained and scrutinized during DE increment.Fig.14 shows that only two high-frequency components, 98th, and 100th components have an incremental growth pattern, which is mentioned in Table VIII. As can be seen in Table V and Table VIII, there are different harmonic components indices for each type of eccentricity that can help distinguishing static from dynamic type by choosing un-common ones. Also, short-circuit in the excitation winding leads to a decrease in the flux density in both half cycles. One can distinguish the only decreasing harmonic components, listed in **Table** that make SC occurrence notable, too.

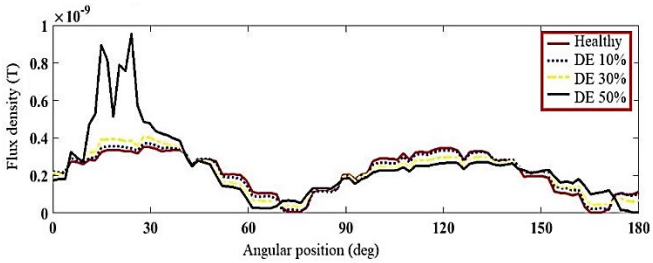

Fig. 13. The flux density of the air gap under dynamic eccentricity

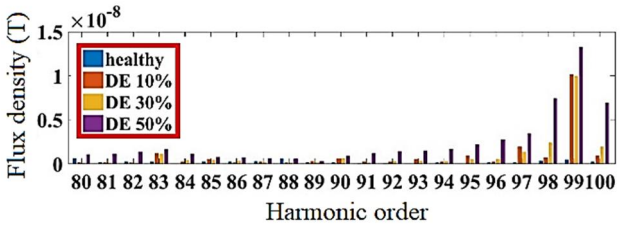

Fig. 14. Flux density amplitude frequency spectrum under dynamic eccentricity.

Table VIII.Flux density amplitude indices for dynamic eccentricity

Fault type	Harmonics order
DE	98, 100
Short-circuit	21,41

VII. CONCLUSION

Static eccentricity fault indices were studied for a sample wound rotor resolver in this paper. The introduced indices could notify static eccentricity fault occurrence and its magnitude by voltage and flux density signals. The big

difference between the faulty and healthy frequency spectrum revealed the fault occurrence affecting the high order harmonics mostly. (The affected harmonics frequency of voltage signals lies between 85- 300 Hz and 150- 450 Hz for flux density signal.

To ensure that the proposed indices are unique, other possible faults were also analyzed. By applying short-circuit and dynamic eccentricity, indices of each were found. Using the uncommon harmonics, the fault type was distinguished from others. Also, the fault magnitude could be calculated using the proposed method. All the analysis was done using the time stepping finite element method. Also, the healthy simulated resolver's accuracy is validated by comparing position error of it and an experimental sample resolver.

Although one may not predict a similar condition in other types of resolvers, this investigation as the first fault diagnosis attempt for resolvers has proved the effectiveness of voltage and flux density signals for this purpose.

References

[1] Z. Nasiri-Gheidari, F. Tootoonchian, "The Influence of Mechanical Faults on the Position Error of an Axial Flux Brushless Resolver without Rotor Windings," IET Electric Power Applications, vol. 11, no. 4, 2017.

[2] R. Alipour-Sarabi, Z. Nasiri-Gheidari, F. Tootoonchian, H.Oraee, "Improved Winding Proposal for Wound Rotor Resolver Using Genetic Algorithm and Winding Function Approach," IEEE Transactions on Industrial Electronics, vol. 66, no. 2, pp. 1325 - 1334, 2019.

[3] H. Saneie, Z. Nasiri-Gheidari, F. Tootoonchian, "Design-Oriented Modeling of Axial-flux Variable-reluctance Resolver Based on Magnetic Equivalent Circuits and Schwarz–Christoffel Mapping," IEEE Transactions on Industrial Electronics, vol. 65, no. 5, pp. 4322-4330, May 2018.

[4] M. Bahari, R. Alipour-Sarabi, Z. Nasiri-Gheidari, and F. Tootoonchian, "Proposal of Winding Function Model for Geometrical Optimization of Linear Sinusoidal Area Resolver," IEEE Sensors Journal, Early Access.

[5] F. Tootoonchian, "Proposal of new windings for 5-X variable reluctance resolvers," IET Science, Measurement & Technology, vol. 12, no. 5, pp. 651 – 656, 2018.

[6] F. Tootoonchian. Z. Nasiri-Gheidari, "Twelve-slot two-saliency variable reluctance resolver with non-overlapping signal windings and axial flux excitation," IET Electric Power Applications, vol. 11, no. 1, pp. 49-62, 2017.

[7] F. Tootoonchian, "Proposal of a New Affordable 2-Pole Resolver and Comparing Its Performance with Conventional Wound-Rotor and VR Resolvers," IEEE Sensors Journal, vol. 18, no. 13, pp. 5284 - 5290, 2018.

[8] A. Daniar, Z. Nasiri-Gheidari, F. Tootoonchian, " Position error calculation of linear resolver under mechanical fault conditions," IET Science, Measurement & Technology, vol. 11, no. 7, pp. 948 - 954, 2017.

[9] F. Zare, Z. Nasiri-Gheidari, F. Tootoonchian, "The Effect of Winding Arrangements on Measurement Accuracy of Sinusoidal Rotor Resolver under Fault Conditions," Measurement, Elsevier, vol. 131, pp. 162-172, 2019.

[10] Z. Nasiri-Gheidari, F. Tootoonchian, "Axial flux resolver design techniques for minimizing position error due to static eccentricities," IEEE Sensors Journal vol. 15, no. 7, pp. 4027 - 4034, 2015.

[11] Z. Nasiri-Gheidari, F. Tootoonchian, F.Zare, "Design-oriented technique for mitigating position error due to shaft run-out in sinusoidal-rotor variable reluctance resolvers," IET Electric Power Applications, vol. 11, no. 1, pp. 132 - 141, 2017.

[12] W. Doorsamy, A. Elyazied Abdallah, W.cronje, L.Dupre, "An Experimental Design for Static Eccentricity Detection in Synchronous Machines Using a Cram´er–Rao Lower Bound Technique," IEEE Transactions On Energy Conversion, vol. 30, no. 1, pp. 254 - 261, 2015.

[13] B.M.Ebrahimi, J.Faiz, B.N. Araabi "Pattern identification for eccentricity fault diagnosis in permanent magnet synchronous motors using stator current monitoring," IET Electric Power Applications, vol. 4, no. 6, pp. 418 - 430, 2010.

[14] B.M. Ebrahimi, J. Faiz, "Diagnosis and performance analysis of three-phase permanent magnet synchronous motors with static, dynamic and mixed eccentricity," IET Electric Power Applications, vol. 4, no. 1, pp. 53 - 66, 2010.

[15] C. Bruzesse, G. Joksimovic, E. Santini "Static eccentricity detection in synchronous generators by field current and stator Voltage Signature Analysis - Part I: Theory," presented at The XIX International Conference on Electrical Machines - ICEM 2010, Rome, Italy 2010.

[16] I. Ahmed, M. Ahmed, K. Imran, et al., "Detection of Eccentricity Faults in Machine Using Frequency Spectrum Technique," International Journal of Computer and Electrical Engineering, vol. 3, no. 1, pp. 1793-8163, 2011.

[17] M. Ahmadi-Darmani, S.M. Mirimani, F.Marignetti, A.Ghaemi Pour, "Static Eccentricity Fault Detection in Flux Switching Permanent Magnet Machines," presented at the International Symposium on Power Electronics, Electrical Drives, Automation and Motion (SPEEDAM), Anacapri, Italy, 2016.

[18] B.M. Ebrahimi, J. Faiz, "Diagnosis and performance analysis of three-phase permanent magnet synchronous motors with static, dynamic and mixed eccentricity," IET Electric Power Applications, 2009.

[19] O. Ogidi, P. Barendse, M. Azeem-khan, "Influence of Rotor Topologies and Cogging Torque Minimization Techniques in the Detection of Static Eccentricities in Axial-Flux Permanent-Magnet Machine," IEEE Transactions on Industry Applications, vol. 53, no. 1, 2017.

[20] N. Rani-Alham, D. Asfani, M. Negara, B.Y. Dewantara, "Analysis of load and unbalance voltage on air gap

eccentricity in the detection of three-phase induction motor," presented at the 2018 International Conference on Information and Communications Technology (ICOIACT), Yogyakarta, Indonesia 2018.

[21] M. Ghods, Z. Nasiri-Gheidari and H. Oraee, "Performance Analysis of Permanent Magnet Vernier Generator underMechanical Faults," International Journal of Industrial Electronics, Control, and Optimization, vol. 1, no. 2, 2018.

[22] H.Saneie, R.Alipour-Sarabi, Z. Nasiri-Gheidari, F. Tootoonchian, "Challenges of Finite Element Analysis of Resolvers," IEEE Trans. Energy Convers, Early Access.

[23] M. Ebrahimi and J. Faiz, "Magnetic field and vibration monitoring in permanent magnet synchronous motors under eccentricity fault," IET Electric Power Applications, vol. 6, no. 1, pp. 35 - 45, 2012.

Shima Tavakoli is born in Tehran, Iran, in 1992. She received her B.S degree from the electrical and computer engineering department of Shahid Beheshti University, Tehran, Iran, in 2015. From 2016 to 2019 she was with advanced electrical motors development center of Niroo Research Institute and received her M.Sc in electrical machines and power electronics from Islamic Azad University, Science and Branch in 2018. She joined the Electrical Machines and Drives institute of Friedrich-Alexander universität in 2019 and is already working toward her Ph.D. in the field of fault diagnosis and predictive maintenance of electrical machines.

Zahra Nasiri-Gheidari received the B.Sc.degree from the IranUniversity of Sciences and Tech-nology, Tehran, Iran, in 2004, and the M.S. and Ph.D. degrees from University of Tehran, Tehran, in 2006 and 2012, respectively, all in electrical engineering. She is currently an Associate Professor with the Department of Electrical Engineering, Sharif University of Technology. Her research interests include design, optimization, and performance analysis of electrical machines and electromagnetic sensors.

.